END
DATE
FILMED
7-80
DTIC

THE ANALYTIC SCIENCES CORPORATION

⑫

LEVEL II

TR-1519-1

PERFORMANCE LOWER BOUNDS
FOR COMPENSATED TRACKING
SENSORS

28 February 1980

Prepared under:

Contract No. N00014-78-C-0684
Task No. NR 274-301

for

NAVAL ANALYSIS PROGRAM
OFFICE OF NAVAL RESEARCH
Department of the Navy
800 N Quincy Street
Arlington, Virginia 22217
(Attn: Mr. James G. Smith, Code 431)

DTIC
S ELECTE D
JUN 17 1980
D

Prepared by:

Jorge I. Galdos
T. Sen Lee

Approved by:

Thomas O. Mottl
Robert F. Brammer

THE ANALYTIC SCIENCES CORPORATION
Six Jacob Way
Reading, Massachusetts 01867

80 6 9 173

ABSTRACT

The process of tracking and localization of a moving acoustic source in the ocean has a natural formulation as a problem in nonlinear filtering theory. In general, the optimal estimator for this signal processing problem cannot be explicitly constructed nor can optimal performance be computed. However, optimal performance can be approximated by using mathematical algorithms which provide lower bounds on attainable estimation accuracy. Lower bounds on tracking and localization errors are especially useful in that they indicate system performance limits and can be computed from basic measurement scenario parameters without reference to specific estimator structure. This report describes the mathematical structure and software required to compute nonlinear filtering lower bounds to the tracking and localization performance attainable with a towed linear acoustic array and a hull-mounted sonar. The state-space model for the acoustic environment and sensor measurement processes used by the lower bound algorithms is also described. Range and bearing estimation performance as a function of signal-to-noise ratio, array distortion, and other important parameters, is studied for a generic measurement scenario.

ACKNOWLEDGEMENTS

THE ANALYTIC SCIENCES CORPORATION

TABLE OF CONTENTS

LIST OF FIGURES

LIST OF FIGURES (Continued)

1.   INTRODUCTION

Estimating the location and track of a moving acoustic source is a basic function in both Navy surveillance and fire control targeting operations. The systems and subsystems which perform these functions have grown increasingly complex and costly, as have the analyses required to evaluate and further develop such systems. Optimization of the performance of such systems is a key to mission and cost effectiveness, and guidelines to attainable performance improvements are of obvious concern.

This report develops a technique termed "nonlinear filtering lower bound performance analysis" as a tool for evaluating limits to passive target tracking and localization performance attainable from a single mobile platform employing up to two target locating sensors: a towed linear acoustic array and a hull-mounted sensor. The techniques presented herein are applicable to both tactical targeting and surveillance scenarios employing passive acoustics.

1.1   STUDY BACKGROUND

The towed linear acoustic array is a key target locating sensor for use in tactical fleet and SSN ASW operations. Used alone or in conjunction with a hull-mounted sonar, the towed array provides tracking and localization data with potential for long range, over the horizon, surveillance and targeting.

New technology developments indicate continuing en-
hancement of performance capabilities through larger aperture
systems (Refs. 1 and 2). However, the realization of such
performance gains may require solution of problems of consider-
able complexity. Calculation of lower bound performance limits
for such systems establishes system accuracy limits against
which system-specific performance estimates and measurements
can be evaluated. Such comparisons serve to define "value-
received" from further investments in performance enhancement
and optimization.

Estimation of the range and bearing of a moving acous-
tic source by one or more spatially distributed sensors can be
formulated as a problem in nonlinear filtering. The nonlinear
filtering approach avoids a number of idealizing assumptions
which have characterized previous studies (Refs. 3-9):

- Linearized analysis

- High signal-to-noise ratio

- Nondynamical (i.e., time invariant) and
  deterministic processes

- Infinite observation intervals

- Ideal (perfect) sensor geometry

- Ideal transmission medium

- Dependence of the results on a specific
  signal processor.

These assumptions are not necessary in the approach used in
this study, and results obtained here are thus free of such
idealizations.

1.2   OBJECTIVES AND APPROACH

The objectives of the work reported herein are:

- To develop nonlinear filtering lower bound performance algorithms suitable to the evaluation of towed-array-based target localization at low as well as high SNR

- To develop stochastic state-space models necessary for the statistical characterization of the acoustic measurement processes and sensors

- To estimate towed array localization performance limits for a representative operational scenario

- To study the effect on localization performance of various important parameters and conditions.

A three-step approach is followed in order to achieve these objectives. First, a stochastic state-space model is derived in order to characterize the physics of the problem. Use of a stochastic modeling approach is particularly suited to evaluation of passive sonar performance in view of inherent uncertainties in predictive models for, and/or experimental data on, the acoustic environment, e.g., transmission loss, ambient nose, arrival structure, signal coherence, etc. and sensor configurations. The availability of powerful modern estimation analysis techniques and related software, together with the signal and noise representations required for the lower bound algorithms, motivates the state-space formulation.

Second, the theory of nonlinear filtering lower bounds is extended so that lower bound analysis is practically applicable to the sonar localization problem. In particular, two discrete-time lower bound algorithms are developed. One

algorithm, based on rate distortion theory, is used to obtain results at low signal-to-noise ratio (SNR). The other algorithm, based on Cramer-Rao theory, is used at high SNR values.

Third, the equations of the state-space model and those of the lower bound algorithm are coded into a computer program. This program is used to generate the numerical results for the specific example considered.

1.3 OVERVIEW

Section 1.4 summarizes the major results obtained in this study. Chapters 2 and 3 present an overview of the theoretical research performed as part of this study. Chapter 2 is addressed to the derivation of a stochastic state-space model that characterizes the physics of the surveillance problem. Chapter 3 describes the extensions in nonlinear filtering lower bound theory required by the surveillance problem. A detailed technical treatment of the material in Chapters 2 and 3 can be found in other documents prepared under the present contract and listed in Section 1.4. In Chapter 4, numerical results obtained by applying the analysis described in Chapters 2 and 3 to a specific surveillance example are presented. Summarizing comments are given in Chapter 5.

1.4 SUMMARY OF MAJOR RESULTS

Principal results developed under the current contract can be summarized as follows:

- **State-Space Model** -- A stochastic state-space model characterizing the time-varying and random dynamics of the surveillance problem has been constructed (See Chapter 2).

- High SNR lower bound -- A nonlinear filtering lower bound algorithm applicable to multidimensional models at high SNR conditions has been derived based on Cramér-Rao theory (see Section 3.3).

- Low SNR lower bound -- A nonlinear filtering lower bound algorithm applicable to low SNR conditions and arbitrary desired functions of the state has been derived based on rate distortion theory (see Section 3.4).

- Numerical results -- For a representative surveillance scenario, range and bearing estimation errors are analyzed as a function of the following parameters and conditions:
  - Signal-to-noise ratio
  - Magnitude of towed array distortion
  - Accuracy of motion compensation
  - Magnitude of initial nominal range
  - Initial localization uncertainty
  - Integration of hull-mounted sonar measurements with towed array measurements (See Chapter 4).

Detailed presentations of the technical development of each of these cited results appear in the following documents issued as part of this contract:

- "A Cramér-Rao Bound for Multidimensional Discrete-Time Dynamical Systems," The Analytic Sciences Corporation Technical Information Memorandum TIM-1519-1 (also issued as a correspondence item in the Feb. 1980 issue of the IEEE Transactions on Automatic Control). See Ref. 13.

- "A Rate Distortion Theory Lower Bound on Desired Function Filtering Error," The Analytic Sciences Corporation Technical Information Memorandum TIM-1519-2 (also to appear as a correspondence item in the IEEE Transactions on Information Theory). See Ref. 14.

- "State Space Models for Sonar System Analysis," The Analtyic Sciences Corporation Technical Information Memorandum TIM-1519-3. See Ref. 12.

- "Nonlinear Filtering Lower Bound Evaluation of Passive Tracking Systems," to appear in the Proceedings of the 1980 IEEE Conference on Acoustics, Speech and Signal Processing (ICASSP). See Ref. 15. A more detailed version of this paper is to be submitted to the IEEE Journal of Oceanic Engineering (Ref. 43).

2.   A STATE-SPACE MODEL FOR
                   ACOUSTIC OCEAN SURVEILLANCE

2.1   INTRODUCTION

A stochastic state-space modeling approach suitable
for passive surveillance sonar system performance evaluation
is presented in this chapter. Uncertainties in predictive
theoretical models and environmental data (random effects/data
authenticity) suggest the utility of this approach, while the
availability of powerful modern estimation and detection analy-
sis techniques (such as the lower bound theory used in this
study) argue for introduction of a state-space formulation.
Specific component models are presented for acoustic transmis-
sion loss, ambient noise, own-ship/source kinematics, and mul-
tiple sensor characteristics.

The physical scenario for the passive surveillance
sonar problem is described in Fig. 2.1-1. A target is assumed
to radiate a single tone which is observed by towed array and
hull-mounted sensors. The range ($R(t)$) and bearing ($B(t)$)
random processes are the two quantities to be estimated from
the observations.

The stochastic state-space model constructed is assumed
to have the form (Ref. 16)

$$\dot{\underline{x}}(t) = F(t)\underline{x}(t) + G(t)\underline{w}(t) \qquad (2.1\text{-}1)$$

$$\underline{y}(t) = \underline{h}(\underline{x}(t),\ t) + v(t) \qquad (2.1\text{-}2)$$
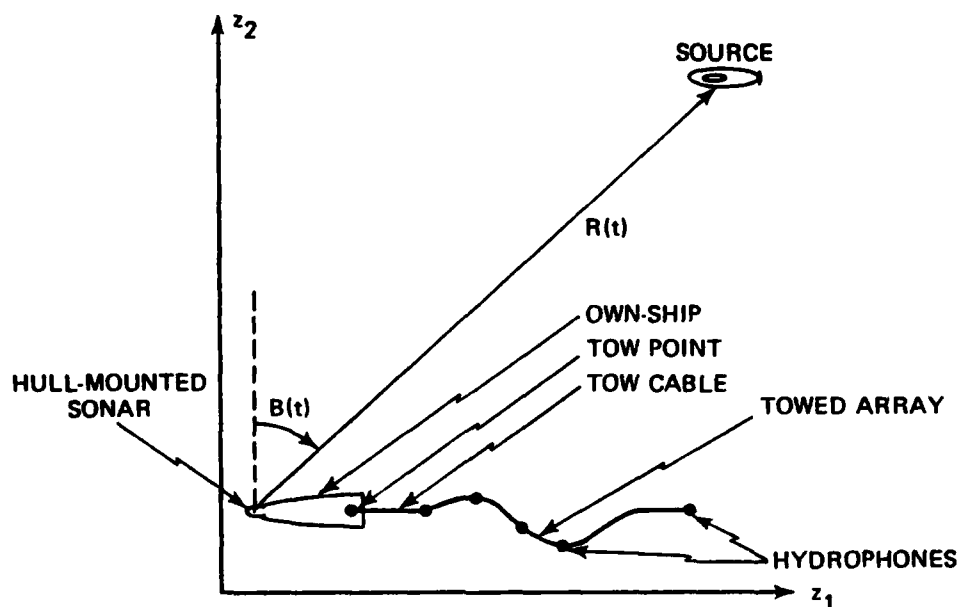
Figure 2.1-1   Surveillance Scenario Geometry

where

$$\underline{x}(t) = \text{system state vector}$$

$$\underline{y}(t) = \text{measurement vector}$$

$$F(\cdot) = \text{system matrix}$$

$$h(\cdot,\cdot) = \text{measurement mechanism}$$

$$w(t), v(t) = \text{independent white Gaussian}$$
$$\text{noise processes.}$$

The components of the time dependent state-vector $\underline{x}(t)$ are used to model acoustic transmission loss, ambient noise, and own-ship/source and towed array kinematics. The vector measurement variable $\underline{y}(t)$ models towed array and hull-mounted sensor measurements. Descriptions of the components of $\underline{x}(t)$ and $\underline{y}(t)$ are presented in the following sections. A detailed technical exposition of the material in this chapter can be found in Ref. 12.

2.2   TRANSMISSION LOSS MODEL

Both ray and wave theories provide deterministic transmission loss predictions for a given sound velocity profile and fixed (non-random) boundary conditions of the ocean. However, deterministic and random variations occur in the ocean sound velocity field in space and time while the ocean surface and bottom are also functions of these same variables. These functional dependencies of the sound velocity field and boundary conditions of the ocean, together with conditional and fundamental uncertainties in any specifications for these variables, suggest that transmission loss be modeled as a stochastic process. In this study a transmission loss model is proposed based on three component models:

- Large scale trends predicted by ray and wave theories

- Small scale behavior; specifically, convergence zone effects and multi-path arrival structure resulting from space/time (random) boundary effects and different transmission paths

- Fluctuations caused by sound velocity field variations.

While the parameters in the model could be estimated from measurement data, for this study parameters are chosen from Refs. 17 and 18.

The first two state-variables $x_1(t)$ and $x_2(t)$ of the state vector $\underline{x}(t)$ are used to model random components of transmission loss. The determinstic trend of transmission loss caused by geometric spreading and absorption is modeled by an algebraic function of the source/receiver range, $R(t)$ (Ref. 17). A sample function of transmission loss generated from

this model is shown in Fig. 2.2-1(a). Other sample functions
of transmission loss taken from Ref. 17 and 18 are shown in
Figs. 2.2-1 (b) and (c) respectively. While these three curves
exhibit similar convergence zone and spreading loss behavior,
the methods for generating each of these curves, and hence
their interpretation, are quite different. The modeling tech-
niques used in these cases are:

- Figure 2.2-1 (a) is derived from the
  constructed stochastic state-space model
  described in this report and is interpre-
  ted as a realization of a stochastic
  process

- Figure 2.2-1 (b) is based on mathematical
  models with model parameter values derived
  from experimental data on convergence
  zone and spreading loss behavior as a
  function of source/receiver range (see
  Ref. 17)

- Figure 2.2-1 (c) is obtained from the
  Parabolic Equation Model for sound propa-
  gation given a specific sound velocity
  profile and set of boundary conditions
  (see Ref. 18).

2.3 AMBIENT NOISE MODEL

The ambient noise model developed here is directed at
frequencies ranging from 100 Hz to 700 Hz. In this frequency
span, there are two distinguishable sources of the ambient
noise field:

- Vertically Anisotropic Ambient Noise -
  Caused primarily by shipping noise in
  the lower frequency regime of the ambient
  noise field

- "True" (ocean generated) Ambient Noise -
  Noise resulting from hydrodynamic effects,
  thermal noise, etc. (dominates the higher
  frequency regime of the ambient noise
  field).
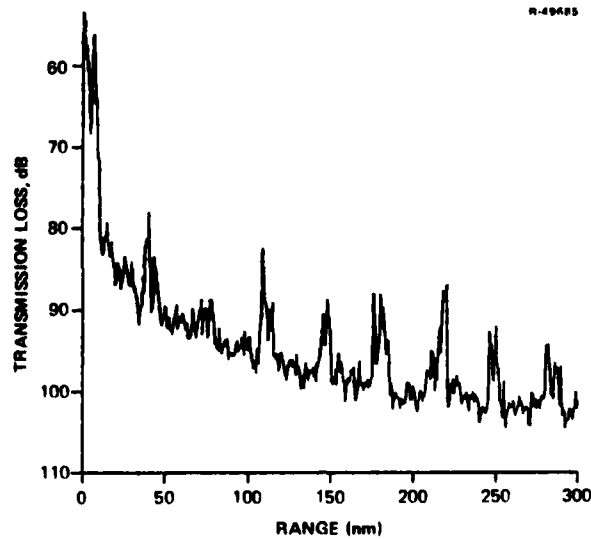
(a) Transmission loss from state-space model
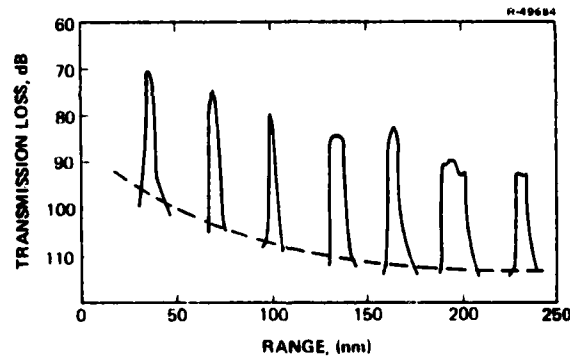
(b) Transmission loss based on mathematical model with
     parameter values derived from experimental data
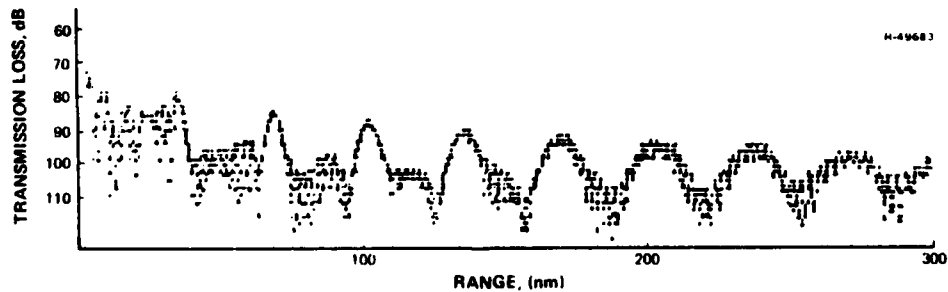
(c) Transmission loss based on numerical solution of
     parabolic equation model

Figure 2.2-1   Sample Functions of Various Transmission
                Loss Models

A variety of ambient noise spectra estimated from
real measurement data are available for the frequency band
considered in this report (see Refs. 17 and 19). Ambient noise
statistics due to shipping are also generally available (see
Ref. 20). However, a state-space representation for ambient
noise is required for applying modern estimation and detection
techniques such as the lower bound analysis used in this study.

The state-space ambient noise model chosen here employs
three state variables ($x_3(t)$ through $x_5(t)$) and is constructed
such that the spectrum of the state-space representation fits
those spectra reported in Ref. 17. A detailed formulation of
the ambient noise state-space model is described in Ref. 12.

For time periods such that the received signal eleva-
tion angle (at own-ship) position remains constant, the ambient
noise can be considered as a stationary process. The reference
ambient noise spectrum is taken from Ref. 17 for the case of
moderate shipping and Beaufort wind force 4 and the spectrum
derived from the state-space model developed here is compared
with the reference spectrum in Fig. 2.3-1. The "match" between
these two spectra for frequencies in the range 100 Hz through
700 Hz is a result of the selection of model parameters. If a
wider frequency band were of concern, the quality of the match
could be extended to a larger frequency range through the intro-
duction of other state variables (modeling additional poles
and zeroes (Ref. 44)).

2.4   OWN-SHIP/SOURCE KINEMATICS MODELS

The own-ship/source kinematics model characterizes
the range, range rate and bearing variables as well as the
range and range rate from the source to each of the towed array
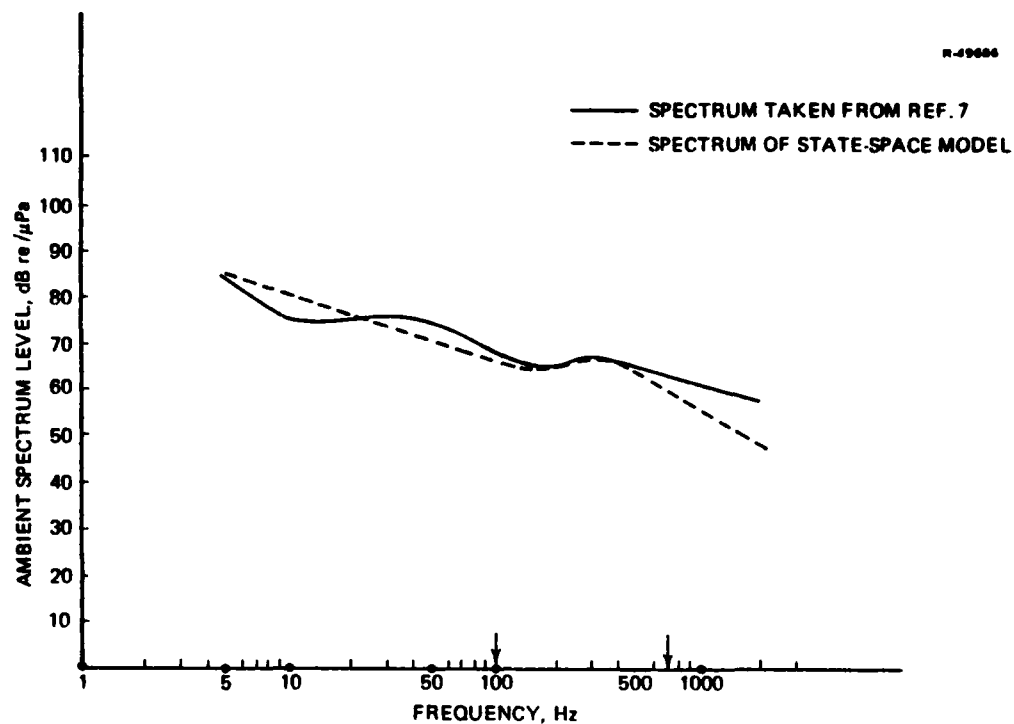
Figure 2.3-1   Ambient Noise Spectra

and hull-mounted sonar sensor elements. These quantities appear
in the models for the transmission loss, doppler shift, array
motion, hull-mounted sonar, and towed array measurements.

Target (source) motion models have received considerable
attention in the literature (e.g., Refs. 21 to 23) in connection
with the structure of tracking filters. The present applica-
tion, however, contains peculiarities which make it different
from other target motion studies:

- A relative motion model is not sufficient
  since the own-ship motion affects the
  towed array dynamics

- Cross-track motion of the own-ship is
  considered to be the more significant
  component for resultant array motion

- It is desirable to have own-ship motion
  characteristics that reflect an attempt
  at minimizing cross-track fluctuations.

A model reflecting these aspects is developed here. By adjust-
ing the model parameters, this model can be used to character-
ize both a surveillance scenario (where neither ship initiates
abrupt maneuvers) or a tactical scenario (where an increased
level of maneuvering is present).

The assumptions used in the derivation of this model
are summarized as follows. Motion is assumed to be planar. A
two-dimensional (z_1, z_2) coordinate system is assumed with the
origin at the location of the own-ship at the beginning of a
signal processing integration interval (time $t = 0$). It is
further assumed that the own-ship has a gyrocompass that does
not experience significant drift during any time interval of
duration equal to $L/V + T$, where L is the combined length of
the tow cable and towed array, V is the magnitude of the mini-
mum velocity of the ship, and T is the integration time. Thus,
the location and orientation of the z_1 and z_2 axes are assumed
to be geodetically fixed.

The own-ship motion is modeled in terms of along-track
(z_1) and cross-track (z_2) components. In the along-track direc-
tion, the ship is assumed to be moving at a uniform speed of
10 kts. In the cross-track direction, own-ship motion is mod-
eled as a low frequency bounded variance process. Such a proc-
ess is obtained here by passing white noise through a second
order low-pass filter with a 7.3×10^{-3} Hz bandwidth. This model
reflects (hypothetical) attempts at minimizing cross-track
fluctuations in the array motion. The RMS level of this proc-
ess is then parametrically varied. A typical own-ship trajec-
tory is shown in Fig. 2.4-1 for an RMS level of 5 ft.

Target motion is also modeled in terms of z_1 and z_2
components. Each of these components has, in turn, two com-
ponents: static and dynamic. The static component is a random
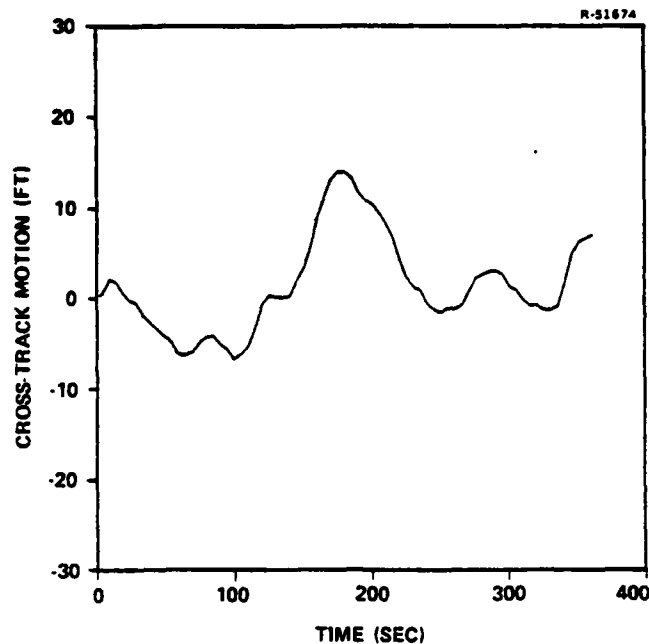
Figure 2.4-1   Typical Own-Ship Trajectory

bias (Ref. 16) and represents the initial (t=0) uncertainty in
the relative position of target and own-ship. The dynamic
component represents the motion of the target during the inte-
gration interval. This latter component is modeled by a second
order Markov process (Ref. 16) with initial position error
equal to zero. The extent of maneuvering is controlled by
adjusting model parameters (such as bandwidths and RMS levels).
Figure 2.4-2 shows a sample trajectory in which the target
moves at an average speed of 10 kts, target maneuvering is
slight, and an initial location uncertainty of 10.5 nm RMS in
each axis (at a nominal range of 35 nm broadside) is used.

2.5   TOW POINT AND TOWED ARRAY MOTION MODELS

Distortion in the linear array geometry can degrade
the directional and range estimating performance capabilities
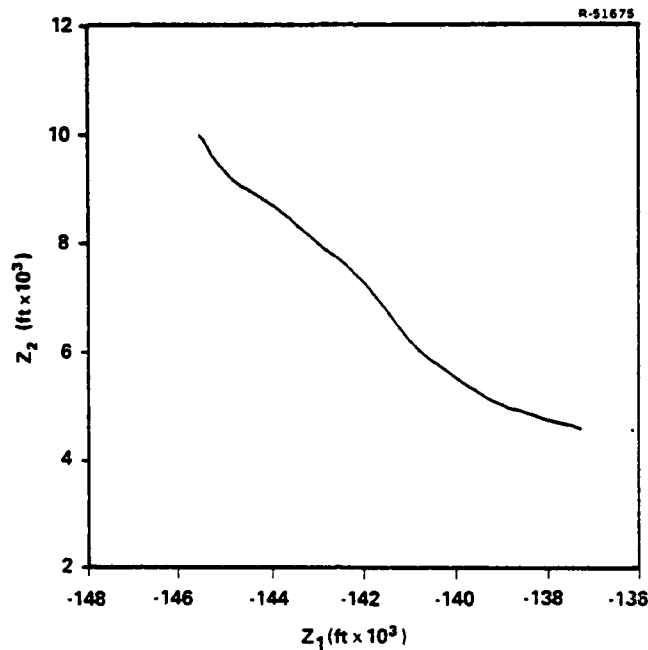
Figure 2.4-2   Typical Target Trajectory

of the towed array. For the surveillance scenario discussed
in this report, the tow ship tries to maintain a straight line
course, implying that the nominal tow point motion contains
only very low frequency and small amplitude components. Follow-
ing the arguments in Refs. 24 and 25, transverse distortion in
the towed array is modeled as obeying a zeroth-order perturba-
tion solution of the Ortloff-Ives equation. This solution
portrays array positional dynamics as perfectly correlated
with those of the ships' tow point, with a time delay depend-
ing upon the physical properties of the towed array, the linear
distance between the tow point and the hydrophones, and the
vessel tow speed.

Two cases of tow point transverse motion are consid-
ered: uncompensated and compensated. In the uncompensated
case, the tow point motion follows the own-ship motion described

in Section 2.4 and illustrated in Fig. 2.4-1. In the compensated
case, the motion of the tow point is assumed to be known up to
the errors in the instruments used to sense tow point motion.
For a Mk 19 gyrocompass and EM log instrumentation suite, the
error in sensing cross-track motion is modeled as the sum of a
ramp and an integrated Markov (see Ref. 24). A sample function
of cross-track tow point position error is shown in Fig. 2.5-1.
The ramp-like nature of the error is evident from this figure.
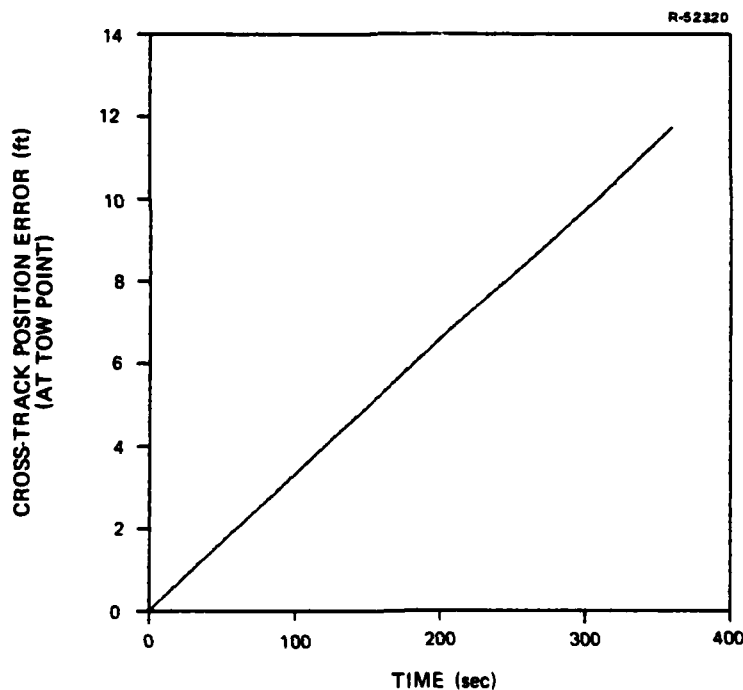
Figure 2.5-1   Sample Tow Point Cross-Track
                Position Error

Measurements taken from the m hydrophones in the towed
array are modeled for the geometry shown in Fig. 2.1-1, and

represented by the variables $y_1(t)$ through $y_{m-1}(t)$. These
measurements are affected by the array motion just described
both in the compensated and uncompensated cases.

2.6   HULL-MOUNTED SONAR MODEL

A representative cylindrical hull-mounted sonar is
shown in Fig. 2.6-1. Each dot in Fig. 2.6-1 represents a sen-
sor element. The characteristics of the sonar are determined
by the diameter, d, the angle between two columns of hydrophone
elements, ϕ, the width of each row of hydrophone elements, h_1,
and the numbers of columns, 2M, and rows, N.

R-45398
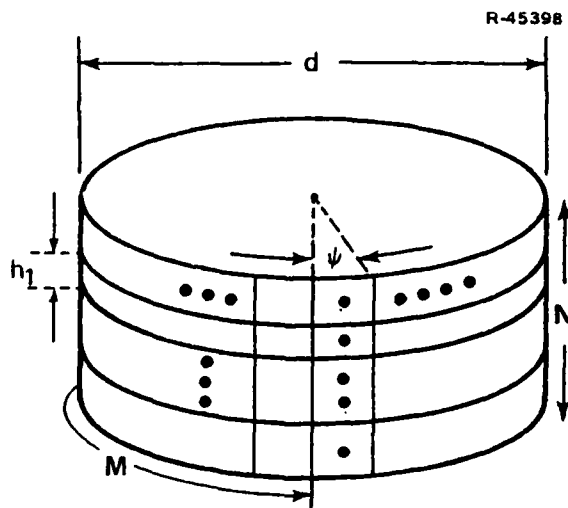
Figure 2.6-1   Cylindrical Hull-Mounted Sonar

Since typical diameters of hull-mounted sonars are
very small compared with the range to be estimated, a split-
beam configuration is nearly optimal according to the argu-
ments in Ref. 26. From the geometry shown in Fig. 2.1-1, the
split-beam measurements from the hull-mounted sonar can be
easily derived, and are represented by the variables $y_{m-1}(t)$
and $y_m(t)$.

3.   FILTERING LOWER BOUNDS FOR SURVEILLANCE SYSTEM PERFORMANCE EVALUATION

3.1   INTRODUCTION

In Chapter 2, the surveillance problem under consideration is defined and cast into the continuous time state-space formulation given in Eqs. 2.1-1 and 2.1-2. This formulation can be transformed into a discrete-time measurement (Ref. 16) expression of the form

$$\dot{\underline{x}}(t) = \underline{F}(t)\underline{x}(t) + \underline{G}(t)\underline{w}(t) \tag{3.1-1}$$

$$\underline{y}(t_k) = \underline{h}(\underline{x}(t_k),\ t_k) + \underline{v}(t_k) \tag{3.1-2}$$

where $t_o \leq t \leq t_k$ and k=1, ..., K. Equation 3.1-1 is a stochastic differential equation defining the time-varying random vector $\underline{x}(t)$ which characterizes the state of the various physical phenomena. Equation 3.1-2 models the discrete time noisy measurements $\underline{y}(t_k)$ available from the various acoustic sensors. The range and bearing random processes are functions of the state specified by

$$R(t) = d_1(\underline{x}(t),\ t) \tag{3.1-3}$$

$$B(t) = d_2(\underline{x}(t),\ t) \tag{3.1-4}$$

where d_1 and d_2 are nonlinear time-varying functions, sometimes called "desired functions" (Ref. 27).

A signal processor for the surveillance problem under consideration can be characterized by functions f_1 and f_2 which define range and bearing estimates, $\hat{R}(t)$ and $\hat{B}(t)$, in terms of the observations $\underline{Y}_0^K = \{\underline{y}(t_o), \ldots, \underline{y}(t_K)\}$,

$$\hat{R}(t) = f_1(\underline{Y}_0^K) \tag{3.1-5}$$

$$\hat{B}(t) = f_2(\underline{Y}_0^K) \tag{3.1-6}$$

In particular, the <u>optimal</u> signal processor, in the sense that it minimizes the mean square error (Ref. 28), is specified by f_1^* and f_2^*,

$$\hat{R}^*(t) = f_1^*(\underline{Y}_0^K) = E\{R(t)\,\big|\,\underline{Y}_0^K\} \tag{3.1-7}$$

$$\hat{B}^*(t) = f_2^*(\underline{Y}_0^K) = E\{B(t)\,\big|\,\underline{Y}_0^K\} \tag{3.1-8}$$

where $E\{\cdot\,|\,\cdot\}$ indicates conditional expectation (Ref. 29). The optimal estimation error

$$\varepsilon_R^*(t) = E\{[R(t) - \hat{R}^*(t)]^2\} \tag{3.1-9}$$

$$\varepsilon_B^*(t) = E\{[B(t) - \hat{B}^*(t)]^2\} \tag{3.1-10}$$

is the smallest error that can be attained by <u>any</u> signal processor.

Because of the nonlinear nature of $\underline{h}$, d_1, and d_2, determination of range and bearing estimates and their associated mean square errors is a problem in <u>nonlinear filtering</u> (Ref. 29). Consequently, the optimal estimators, specified by Eqs. 3.1-7 and 3.1-8, and the optimal performance, specified by Eqs. 3.1-9 and 3.1-10, cannot be computed in general (Ref. 10). One is then forced to turn to one of the large number of sub-optimal filtering techniques that have appeared in the literature (e.g., Refs. 16 and 29) and to approximate the optimal performance by lower bounds.

Lower bounds are time functions such as $\varepsilon_{R,LB}(t)$ and $\varepsilon_{B,LB}$, which obey the relations

$$\varepsilon_{R,LB}(t) \leq \varepsilon_R^*(t) \qquad (3.1\text{-}11)$$

$$\varepsilon_{B,LB}(t) \leq \varepsilon_B^*(t) \qquad (3.1\text{-}12)$$

Lower bounds are considered to be <u>tight</u> when they tightly bound, and thus closely approximate, the optimal errors. Lower bounds have the important feature that their computation is <u>independent of signal processor design</u>. Thus, in order to compute lower bounds, one does not need to design a signal processor. Consequently, tight lower bounds can be used to

- Evaluate fundamental limitations of sur-
  veillance system performance (before
  designing a signal processor);

- Judge how close to optimal a particular
  signal processor is and thereby deter-
  mine how much performance improvement is
  possible;

- Assess when further signal processor
  design effort is not cost effective.

3.2 PREVIOUS WORK

Several researchers have investigated the surveil-lance problem area (e.g., Refs. 3-9). However, in order to obtain tractable results, these investigators always invoke several of the following assumptions:

- Validity of linearized analysis

- High signal-to-noise ratio and infinite
  observation time

- Non-dynamic (i.e., time invariant) and deterministic behavior

- Perfect array geometry

- Ideal transmission medium

- Specific signal processor.

These restrictive assumptions are not necessary in the analysis reported in this study; their significance, and the approach used to avoid them, are addressed in the following six paragraphs.

Validity of Linearized Analysis Several investigators have assumed the validity of linearized analysis in the study of the passive surveillance problem. Results based on linearized analysis are often optimistic, highly dependent on the selection of the linearizing trajectory, or not valid if the nonlinearities are severe relative to the fluctuations about the assumed operating point. In-particular, a rather high SNR is usually required for linearized analysis to be valid (Ref. 31). An example of linearized analysis is given in Ref. 3 where the covariance of an extended Kalman filter (Ref. 16) is used for analyzing the performance of a passive surveillance system. The resulting range and bearing accuracies are extremely small and thus appear to be optimistic. In constrast, the approach in the present study uses the actual nonlinear dynamics of the problem (i.e., linearization is not used).

High Signal-to-Noise Ratio In addition to techniques based on linearization, the Cramér-Rao inequality for parameter estimation (Ref. 27) has been used by some investigators in the analysis of surveillance systems (e.g., Ref. 4). However, it is well known that, in the nonlinear low SNR region of receiver operation, bounds based on the Cramér-Rao inequality

are not tight (Refs. 27 and 28). For passive sonar surveillance applications, low SNRs are often encountered (Ref. 32). In the present study, this difficulty is overcome by deriving a lower bound (based on Ref. 10) which is most tight at low SNR, as described in Section 3.3. Furthermore, in order to obtain tight bounds at high as well as low SNR, new results based on Cramér-Rao theory are derived, as described in Section 3.4.

Non-Dynamic Behavior In the surveillance problem considered in this study, the target source as well as the sensor array are typically in motion. Thus, one is interested in estimating random processes such as R(t) and B(t) rather than random parameters. The behavior of these processes can be naturally modeled as stochastic dynamical systems. However, in order to simplify the analysis or apply the Cramér-Rao bound for parameter estimation, previous investigators have often used static parameters, often in conjunction with infinite observation time intervals, to model the physical variables. In the present study, this restriction need not be imposed since dynamical system lower bound techniques are used.

Perfect Array Geometry When a linear array sensor is towed through the water, the locations of the sensor elements deviate from the ideal straight-line configuation. Perfect alignment of the sensor elements has been an assumption in previous studies. It has been shown that distortions in the geometry of a linear array can occur and do contribute significantly to estimated range error (Refs. 2, 9 and 24). In the present study, distortions of the linear array are included and are modeled by a low-order perturbation of the solution to the Paidoussis equation (Ref. 30) for a flexible slender cylinder in axial flow, as done in Ref. 24.

Ideal Transmission Medium - The complex nature of the
ocean as a transmission medium for sound is well known (e.g.,
convergence zones, multipath arrival structure, random varia-
tions in space/time etc., Ref. 34); however, this complex be-
havior has often been simplified and/or neglected in studies
of acoustic array performance. In this study, variations in
transmission loss are described by a parametric stochastic
model as described in Chapter 2.

Specific Signal Processor - Surveillance system per-
formance is often evaluated by assuming a specific signal proc-
essor structure. This approach requires the potentially costly
design of the signal processor. Furthermore, the performance
results obtained are dependent on the nature of the signal
processor used. In contrast, lower bound performance evalua-
tion does not involve a design effort and the results are not
limited to a specific signal processing method.

3.3   LOW SIGNAL-TO-NOISE LOWER BOUND

In order to achieve the objectives of this study, it
is required to have a performance bound algorithm which is
applicable to the surveillance problem and is tight at low SNR.
Thus, an algorithm must be available which yields a lower bound
on the optimal range and bearing errors as defined in Eqs.
3.1-9 and 3.1-10.

Lower bounds based on rate distortion theory (Refs.
35 and 36) have been found to be tight in the low SNR region
of receiver operation (Ref. 27 and 34). In Ref. 10, a rate
distortion theory lower bound is derived for stochastic state-
space models such as the one under consideration here. The
bound in Ref. 10 is applicable to a general nonlinear filter-
ing problem and thus includes nonstationary, multidimensional

processes and signals, and is also applicable to sampled data (discrete time) as well as analogue (continuous time) measurements. However this bound is derived for the mean square error measure

$$\varepsilon_K^* = \sum_{i=1}^{n} w_i E(x_{i,K} - \hat{x}_{i,K}^*)^2 \qquad (3.3\text{-}1)$$

where w_i are positive weighting constants, $x_{i,K}$ denotes the ith component of the state $\underline{x}_K$ and $\hat{x}_{i,K}^* = E(x_{i,K}|\underline{Y}_0^K)$ is the optimal estimate of $x_{i,K}$.

The performance index in Eq. 3.3-1 is not useful for the surveillance problem under consideration. In this problem, it is necessary to evaluate the errors in range and bearing (Eqs. 3.1-9 and 3.1-10). Range and bearing are nonlinear desired functions of the state, as shown in Eqs. 3.1-3 and 3.1-4. Furthermore, the algorithm in Ref. 10 requires the computation of the entropy (Ref. 35) of the state vector. This computation can be very costly.

As part of this study, a new lower bound algorithm has been derived in Ref. 13. This new algorithm extends the development in Ref. 10 in three directions. First, the algorithm derived here is applicable to arbitrary desired functions of the state, such as d_1 and d_2 in Eqs. 3.1-3 and 3.1-4. Second, the computational problem of evaluating the entropy of a vector is replaced with the more tractable task of evaluating the entropy of a scalar random variable. Third, the new algorithm has the option of bypassing the Jensen inequality (Ref. 35) used in Ref. 10, allowing a tighter bound to be obtained at the expense of additional computations.

3.4 HIGH SIGNAL-TO-NOISE LOWER BOUND

In order to obtain tight performance bound results at high as well as low SNR, an algorithm based on Cramér-Rao theory and applicable to the surveillance problem under consideration is needed. Results of previous research (Ref. 36) on the use of Cramér-Rao theory for nonlinear filtering problems are limited to scalar (i.e., one-dimensional) state-space models and require a positive process noise covariance (Ref. 39). The surveillance model under consideration here, however, is multidimensional and has some zero entries in the process noise covariance matrix (i.e., the covariance matrix is singular, Ref. 16).

As part of this study, a new lower bound algorithm based on Cramér-Rao theory and applicable at high SNR has been derived in Ref. 13. This new algorithm extends the development in Ref. 36 in three directions. First, the lower bound algorithm is applicable to multidimensional systems. Second, the results apply to the case where the process noise covariance is singular. Third, the new algorithm is as tight, and in some cases tighter, than that in Ref. 36. The derived algorithm can be used in the analysis of desired function errors, such as range and bearing errors (see Eqs. 3.1-3 and 3.1-4), by applying the formula for desired function parameter estimation given in Ref. 27.

3.5 SUMMARY OF COMPUTER SOFTWARE

In order to obtain numerical results using the state space model described in Chapter 2 and the nonlinear filtering algorithms discussed in this chapter, a number of interacting computer modules have been developed as part of this study. The overall software structure is summarized in Fig. 3.5-1.

R-49687

```
                                      ┌──────────────────┐
                                      │  HIGH SNR BOUND  │────► εR, LB
                                      │    ALGORITHM     │
                                      │                  │────► εB, LB
                                      └──────────────────┘
                                        ▲              ▲
   ┌──────────────┐   ┌──────────────┐   ┌──────────────┐
   │  SIMULATED   │   │ TOWED ARRAY  │   │ HULL-MOUNTED │
   │DATA GENERATION│─►│ MEASUREMENT  │─► │    SONAR     │
   │  (TRIAN TM)  │   │    MODEL     │   │ MEASUREMENT  │
   └──────────────┘   └──────────────┘   │    MODEL     │
                                          └──────────────┘
   ┌──────────────┐   ┌──────────────────────────────┐
   │   ENTROPY    │◄─►│        LOW SNR BOUND         │────► εR, LB
   │ COMPUTATIONS │   │         ALGORITHM            │
   └──────────────┘   │                              │────► εB, LB
   ┌ ─ ─ ─ ─ ─ ─ ┐   └──────────────────────────────┘
     JENSEN           ▲
   │ INEQUALITY │◄────┘
     BYPASS
   └ ─ ─ ─ ─ ─ ─ ┘
```
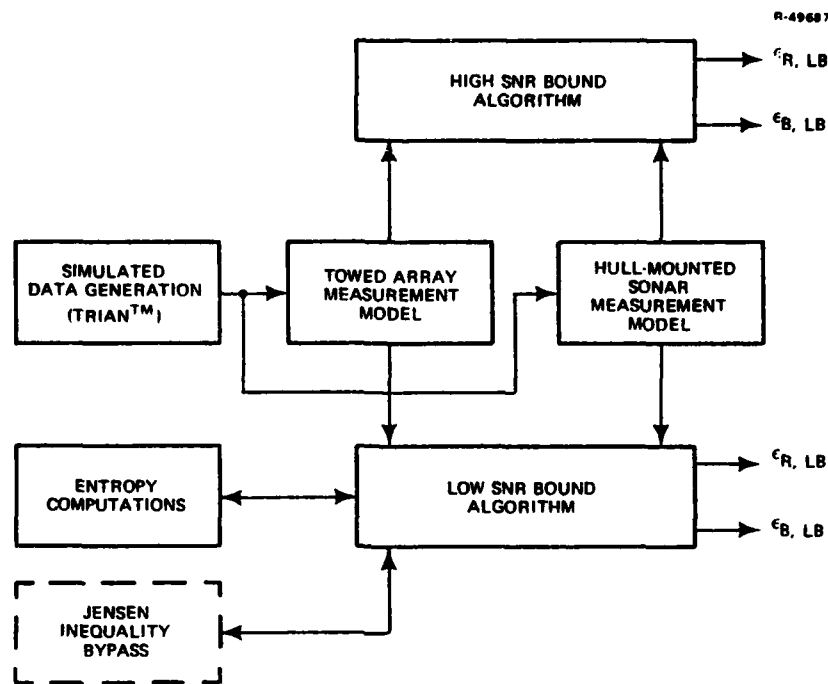
Figure 3.5-1   Overall Software Structure for Lower
                 Bound Evaluation

Not shown in Fig 3.5-1 are the subcomponents of each of the
blocks, as well as the tape and disk storage facilities.

Generation of the necessary Monte Carlo simulated
data is accomplished using TRIAN^{TM} software. A module contain-
ing the equations for the state dynamics given in Chapter 2 is
linked with TRIAN^{TM} during the data generation phase. The
generated data is used in the high as well as the low SNR Lower
Bound Modules. These algorithms are linked with modules speci-
fying the various measurement models.

TRIAN is a trademark of The Analytic Sciences Corporation.

The low SNR algorithm requires the evaluation of the entropy of the range and bearing. This computation uses the probability density function of range and bearing (which in the general case is computed in the entropy module), the associated confidence intervals (Ref. 38), and a weighted maximum-likelihood criteria (Refs. 39 and 40). In the special case where the distribution of the variables is theoretically known, the entropy model uses this latter information. In addition to the entropy module, the low SNR algorithm has the option of being linked with the Jensen inequality bypass module. This latter module is drawn in Fig. 3.5-1 using a broken line indicating that it is not presently implemented.

4. SURVEILLANCE SYSTEM PERFORMANCE EVALUATION

4.1 INTRODUCTION

In this chapter, the surveillance scenario described in Section 2.1 is analyzed using the lower bound computer program described in Section 3.5. The objective of the analysis is to evaluate the effect on surveillance system performance of the following key parameters and conditions:

- Towed array distortion (Section 4.2)

- Motion compensation quality (Section 4.2)

- Magnitude of nominal range (Section 4.3)

- Initial target location uncertainty (Section 4.4)

- Inclusion of hull-mounted sonar measurements (Section 4.5)

Extensions of these results are considered in Section 4.6.

In each of the above cases, plots of range and bearing RMS error, as given by the low SNR rate distortion (RD) based lower bound (Section 3.3) and the high SNR Cramér-Rao (CR) based lower bound (Section 3.4), are given as a function of SNR. Range RMS error is plotted in dB re 1 ft. Bearing RMS error is plotted in dB re 1 rad. SNR, in dB, is taken to be the signal-to-noise ratio at an individual hydrophone and is computed according to

$$SNR = 10 \log_{10} \left\{ \frac{\text{Signal average power}}{\text{Noise power in a 1 Hz band centered at the carrier frequency}} \right\} \quad (4.1\text{-}1)$$

Because of the narrow-band nature of the signal, noise spectra can be assumed to be flat in the vicinity of the carrier frequency. Thus, white noise is used to model the effect of ambient as well as front-end receiver noise.

The following conditions are used in all cases:

- Number of hydrophones in towed array = 20

- λ = wavelength of signal = 500 ft

- Hydrophone spacing = $\lambda/2$

- Array length = 10 λ

- Data rate = 20 samples/sec

- Observation interval = 5 sec

- Target nominally broadside to towed array

- Nominal range = 35 nm (unless otherwise stated)

- Initial target location uncertainty = 10.5 nm in each (z_1 and z_2) axis (unless other wise stated)

- Convergence zone width = 4 nm

- Number of Monte Carlo trials = 50

In Sections 4.1 to 4.5, it is assumed that measurements are taken with only the towed array whereas in Section 4.6 it is assumed that measurements are taken with both the towed array and the hull-mounted sonar sensors.

4.2 EFFECT OF TOWED ARRAY DISTORTION AND MOTION COMPENSATION

In Figs. 4.2-1 and 4.2-2, range and bearing error are plotted as a function of SNR for the following three conditions:
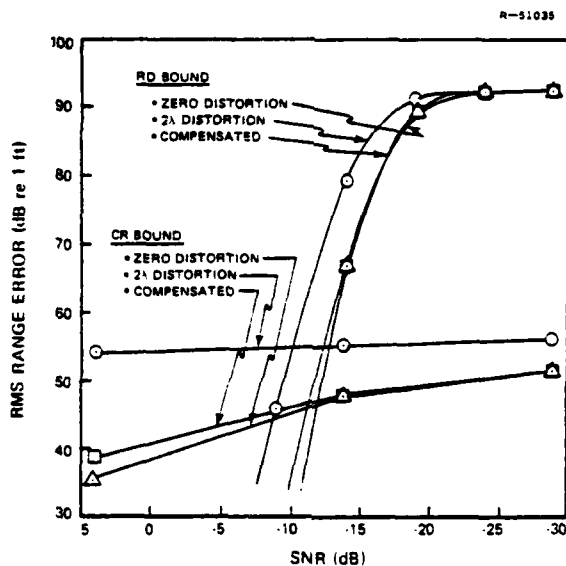
Figure 4.2-1   Effect of Array Distortion and Motion
Compensation on Range Error as a Function
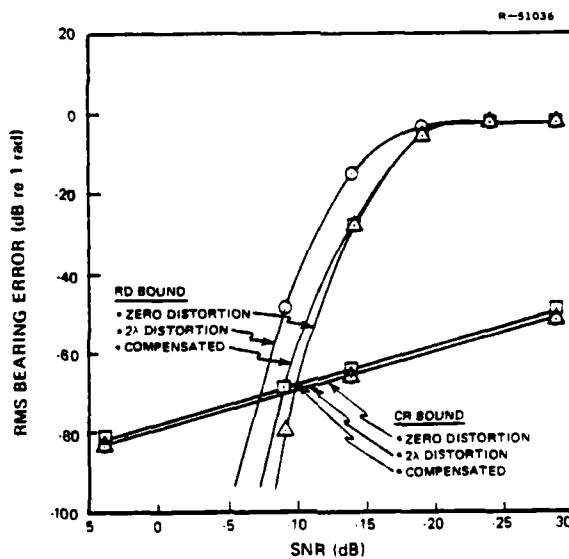on SNR (RD = Rate Distortion, CR = Cramér-
Rao)

Figure 4.2-2   Effect of Array Distortion and Motion
Compensation on Bearing Error as a
Function of SNR

4-3

- Zero array distortion (perfect linear geometry)

- Array distortion with RMS level of 2 λ

- Compensated array distortion.

The zero array distortion condition models the ideal case in which either all hydrophones are perfectly aligned or error-free motion compensation is achieved. The 2 λ array distortion condition represents a worst-case hydrophone misalignment (for the 10 Hz signal used in the simulation 2λ = 1000 ft). However, for a higher signal frequency such as 250 Hz (λ = 20 ft), the 2 λ RMS distortion level may not be unusual. The compensated array distortion condition assumes the use of a Mk 19 gyrocompass - EM log motion sensing instrumentation suite, described in Section 2.5, which makes hydrophone misalignment independent of array distortion.

It is seen in Figs. 4.2-1 and 4.2-2 that <u>in all cases the RD-based bound is significantly tighter at low SNR, whereas the CR-based bound is significantly tighter at high SNR. This behavior is found in all the various conditions considered in this chapter</u>.

At <u>high SNR</u> the CR bound results indicate that, as expected (Refs. 8 at 9), array distortion has a severe detrimental effect on range but not on bearing error. In fact, the small slope of the range error curve for the 2 λ distortion case indicates an <u>"array-distortion-limited behavior"</u> since improvements in SNR have little effect in reducing range error. This behavior is not observed for bearing error. Motion compensation significantly reduces the effect of array distortion on range error. Motion compensation, however, increases the bearing error slightly, possibly because the ramp-like characteristic assumed for the motion compensation errors introduces a (random) bearing bias.

At <u>low SNR</u>, the RD bound results show in all cases a
threshold effect (typical of angle modulation systems). Array
distortion shifts the location of the threshold and a <u>"noise-
limited behavior"</u> is observed. The assumed motion compensa-
tion significantly reduces the effect of array distortion on
both range and bearing errors. Note that as the SNR is de-
creased below -20 dB, no further deterioration in performance
is shown by the RD bound, indicating that measurements no longer
contain significant information and consequently an estimator
must rely on the a priori estimate.

Two other conditions were studied. First, in order
to explore the adequacy of the gyrocompass instrument assumed
in the motion compensation, the magnitude of the Mk 19 errors
were reduced by a factor of ten while leaving EM log errors
unchanged. The resulting range and bearing errors (not shown
here) essentially coincide with those resulting from Mk 19
compensation, indicating that further improvements in motion
compensation quality will not result from improvements in the
gyrocompass instrument.

Second, in order to assess the effect of smaller array
distortion, the rms level of array distortion was reduced to
$\lambda/8$. The resulting range and bearing errors (not shown here)
essentially coincide with the zero array distortion case.
This indicates that for this level of distortion no significant
performance degradation would occur if an optimal processor
were realizable.

4.3   EFFECT OF NOMINAL RANGE

In Figs. 4.3-1 and 4.3-2, range and bearing error are
plotted as a function of SNR for the following two conditions:
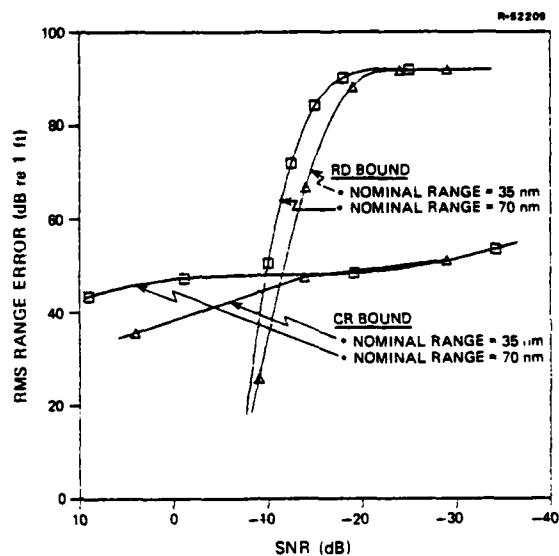
Figure 4.3-1   Effect of Nominal Range on Range Error
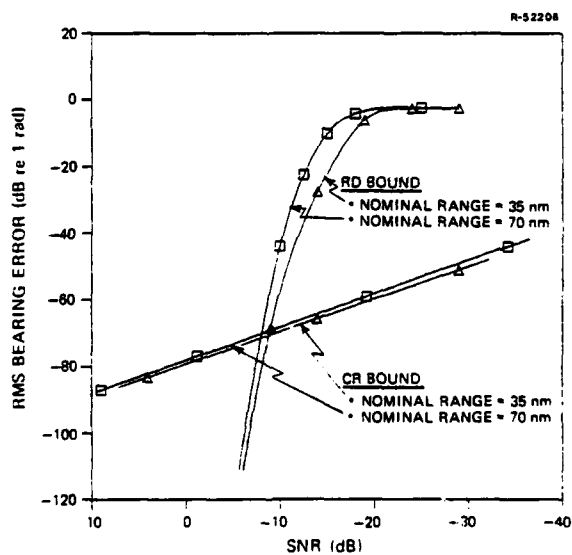as a Function of SNR

Figure 4.3-2   Effect of Nominal Range on Bearing Error
as a Function of SNR

- Target at a nominal range of 35 nm
  (first convergence zone)

- Target at a nominal range of 70 nm
  (second convergence zone)

In both cases, the initial target location uncertainty (i.e., the RMS error in the target location before any measurements are processed) is assumed to be 10.5 nm in each axis. In addition, in order to study the effect of increased nominal range, zero array distortion (or perfect motion compensation) is assumed.

Range error shows some sensitivity to nominal range at both low and high SNR. This sensitivity is in the direction expected: <u>as nominal range is decreased, the curvature of the wavefront can be better measured by the array and consequently smaller range errors are obtained</u>. Bearing error, however, shows significantly less sensitivity than range error, particularly at high SNR.

4.4 EFFECT OF INITIAL TARGET LOCATION UNCERTAINTY

In Figs. 4.4-1 and 4.4-2, range and bearing error are plotted as a function of SNR for the following two conditions:

- Initial RMS target location error = 30%
  of nominal range (each axis)

- Initial RMS target location error = 60%
  of nominal range (each axis)

In both cases the nominal range is taken to be 35 nm (first convergence zone). In addition, in order to study the effect of initial target location error, zero array distortion (or perfect motion compensation) is assumed.
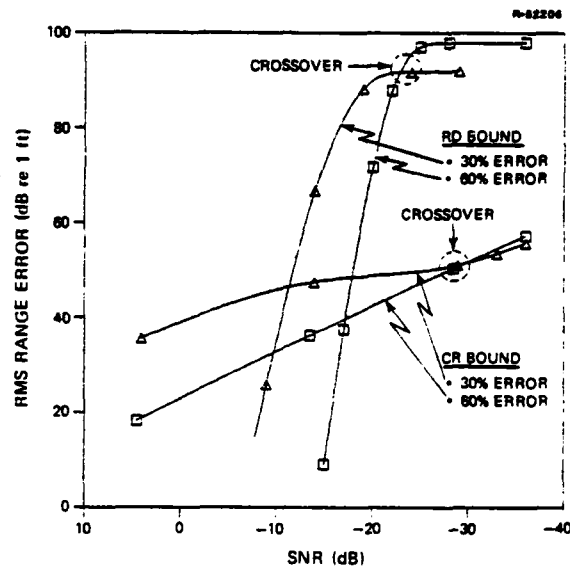
Figure 4.4-1   Effect of Initial Target Location Uncertainty
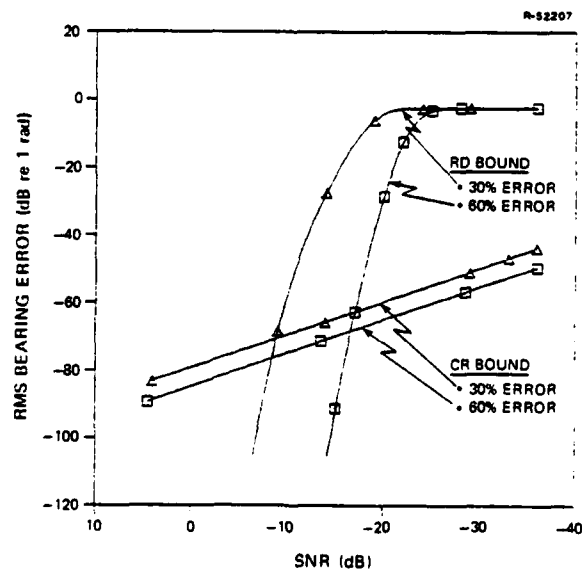on Range Error as a Function of SNR

Figure 4.4-2   Effect of Initial Target Location Uncertainty
on Bearing Error as a Function of SNR

It is seen from Figs. 4.4-1 and 4.4-2 that, except at very low SNR, both range and bearing error exhibit an unusual behavior: the smaller initial location uncertainty produces the larger range and bearing error. At very low SNR, range error shows a crossover (see Fig. 4.4-1), so that the smaller initial location uncertainty produces the smaller range error.

This behavior for the range error curves shown in Fig. 4.4-1 can be explained by observing the interplay of three underlying principles:[*]

1) Estimates are a mix of a priori information and measurement information. In particular:

   ● Except at very low SNR, range estimates are more heavily based on the measurements than on the a priori initial location information

   ● At very low SNR, measurements contain very little information and therefore estimates are heavily based on the a priori initial location information.

2) Range error performance varies nonlinearly with range to the target. In particular:

   ● For distant target locations (e.g., in the cross-hatched area of Fig. 4.4-3), range error performance deteriorates somewhat with increasing range (see Fig. 4.3-1)

   ● For target locations close to the array (e.g., in the shaded area of Fig. 4.4-3), wavefront curvature is more pronounced and consequently significantly smaller range error is obtained.

---

[*]Similar observations can be made regarding the bearing error curves shown in Fig. 4.4-2.
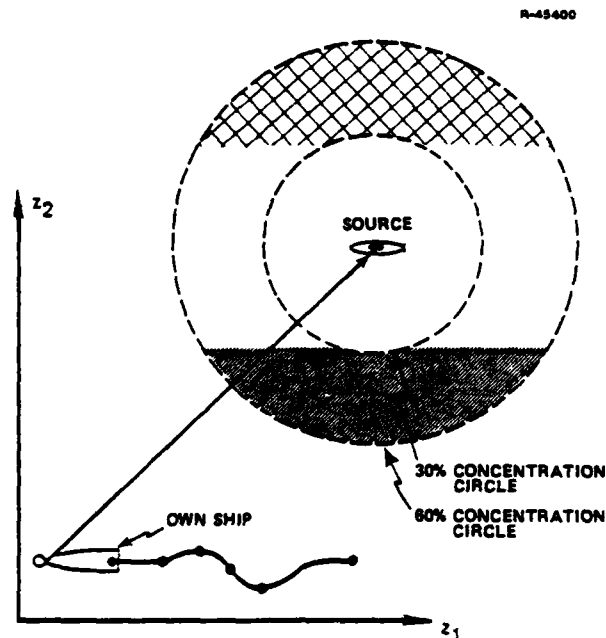
Figure 4.4-3   Concentration Circles for Target Locations
(Note: Figure not drawn to scale)

3) <u>Target location uncertainty specifies the dis-
tribution of possible target locations for rms
error computation</u>.   In particular (see Fig.
4.4-3):

●   The assumption of a 30% target location
uncertainty implies that the ensemble of
possible target locations is concentrated
inside the 30% concentration circle.   A
similar statement holds for the 60% tar-
get location uncertainty.

●   RMS error performance, used in this study,
is an average of the estimation error
which occurs at a specified SNR over all
possible target locations.

When target locations are distributed in the 60% cir-
cle (and when SNR is sufficiently high so that estimates are
determined by the measurements), estimation errors correspond-
ing to target locations in the shaded region in Fig. 4.4-3 are

small enough to produce a significant decrease in rms error.
In contrast, target locations in the cross-hatched area of
Fig. 4.4-3 have a less pronounced effect on the rms error.

From an operational viewpoint, these results indicate
that if a target can be anywhere in the 60% region and if noise
levels are sufficiently small, then a small range error can be
expected. Note that the results displayed on Figs. 4.4-1 and
4.4-2 are a consequence of <u>the ability of the lower bound tech-
niques to account explicitly for nonlinearities. Linearized
analysis would have led to the opposite conclusions</u> since in
linearized analysis range and bearing error vary in direct
proportion to initial location error.

At very low SNR, it is seen that the range error curves
(see Fig. 4.4-1) show a crossover. This behavior occurs be-
cause at very low SNR, measurements contain very little informa-
tion and consequently an estimator must rely on the a priori
estimate. The error in the a priori estimate is, of course,
larger for the case of 60% initial error. Consequently, at
very low SNR, range errors corresponding to the 60% initial
error assumption are larger than those corresponding to the
30% assumption.

4.5   EFFECT OF HULL-MOUNTED SONAR DATA AVAILABILITY

In Figs. 4.5-1 and 4.5-2, range and bearing error are
plotted as a function of SNR for the following two conditions:

- Only towed array (TA) measurements are
  processed

- Towed array measurements combined with
  hull-mounted sonar (HMS) measurements
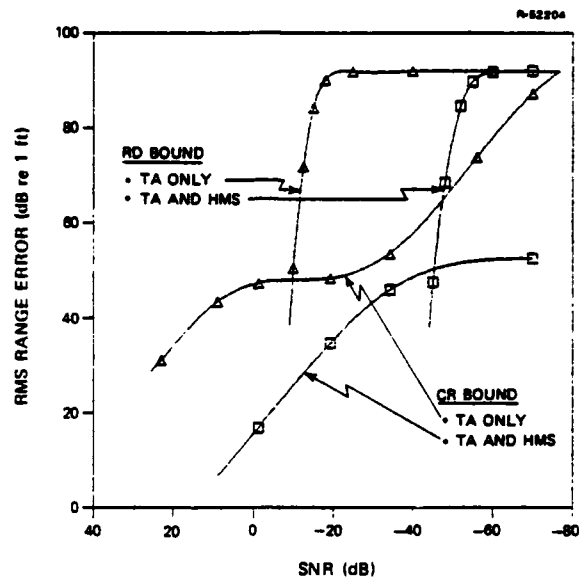 are processed.

Figure 4.5-1   Effect of Hull-Mounted Sonar on Range
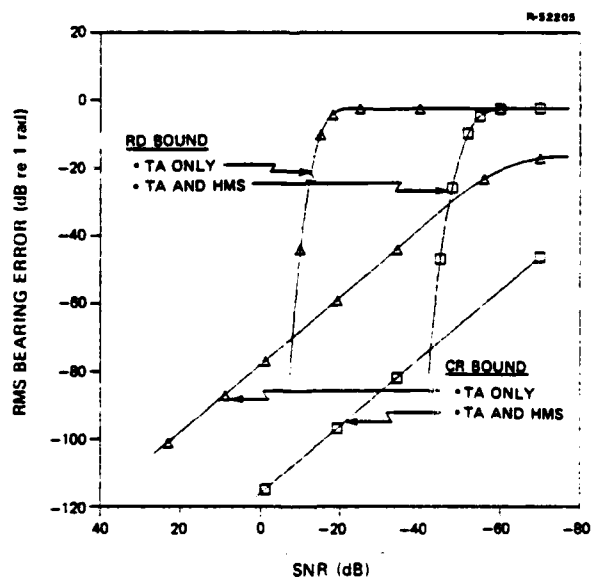Error as a Function of SNR

Figure 4.5-2   Effect of Hull-Mounted Sonar on Bearing
Error as a Function of SNR

In both cases the nominal range is taken to be 70 nm (second convergence zone), the initial location uncertainty is taken to be 15% of the nominal range in each axis, and zero array distortion (or perfect motion compensation) is assumed. In addition, it is assumed that the length of the tow cable is 3000 ft, the length of the tow ship is 400 ft, and that $M = 36$ and $N = 7$ in Fig. 2.6-1 so that 504 hydrophones in a split beam configuration make up the hull-mounted sonar measurements.

The inclusion of the hull-mounted sonar is seen to have two effects on range and bearing errors. First, at high SNR (40 dB > SNR > 0 dB, approximately), performance improves by up to 35 dB. Second, the threshold region is displaced to the right, from SNR $\sim$ 0 dB to SNR $\sim$ -40 dB. As a result of this second effect, range and bearing estimation performance improves dramatically (up to 50 dB for range and 90 dB for bearing) in the region 0 dB > SNR > -40 dB.

In interpreting these results, it should be emphasized that the hull-mounted sonar is assumed to include 504 hydrophones whereas the towed array is assumed to have only 20 sensors. If the towed array were modeled as having more than 20 hydrophones, then the inclusion of the hull-mounted sonar may produce a smaller change in performance.

4.6 SUMMARY AND EXTENSIONS

In this chapter, the capabilities of the lower bound algorithms developed in this study are demonstrated in terms of a specific surveillance example. Results are presented for range and bearing estimation error performance as a function of SNR and other key parameters and conditions (towed array distortion, motion compensation quality, magnitude of nominal

range, initial target location, and inclusion of hull-mounted
sonar data). Some of the results obtained differ radically
from those predicted by linearized analysis, indicating the
importance of explicitly modeling nonlinearities in order to
prevent some of the pitfalls inherent in linearizations.

The results presented assume the nominal parameters
and conditions listed in Section 4.1. In particular, it is
assumed that the towed array has 20 hydrophones and that 100
measurements (5 second data record at 20 samples/sec) are made
with each hydrophone. In practice a larger number of hydro-
phones and measurements will be encountered. Increasing the
number of hydrophones and measurements is expected to affect
performance in a manner analogous to the introduction of the
hull-mounted sonar analyzed in Section 4.5:

- Improved performance at low SNR

- Greatly improved performance at inter-
  mediate SNR produced by a shift in the
  threshold region toward lower SNR values.

The quantitative form of these effects remains to be deter-
mined.

5.   SUMMARY

Estimating the location of a moving acoustic source
is an important function in both Navy surveillance and fire
control targeting operations. The analysis of attainable track-
ing localization (range and bearing) rms error is the subject
of this report. The methodology and results presented herein
can be used to assess surveillance and tracking system accuracy
and to establish realistic signal processor design objectives.

The surveillance scenario considered here has a distant
randomly moving target which is assumed to radiate a single-tone
acoustic signal. This signal is observed by a single platform
equipped with two sensors: a towed array subject to dynamic
deformations, and a hull-mounted sonar.

The problem of estimating range and bearing to the
target can be formulated as a nonlinear filtering problem.
Consequently, the optimal estimator cannot in general be con-
structed nor can the optimal performance be computed. Optimal
performance, however, can be approximated using the technique
of nonlinear filtering lower bound analysis. This technique
avoids a number of idealizing assumptions which have been in-
voked in previous studies:

- Validity of linearized analysis

- High signal-to-noise ratio (SNR)

- Time-invariant and/or non-stochastic
  behavior

- Infinite observation intervals

- Ideal (non-deformed) towed array geometry

- Ideal transmission medium

- Dependence of the results on a specific signal processor design.

In contrast to lower bound techniques for parameter estimation, nonlinear filtering lower bounds have not previously been applied to practical problems such as the surveillance application considered here.

The primary objectives of the work reported on here are to extend the theory of nonlinear filtering lower bound analysis in order to make it applicable to the surveillance localization problem, and to apply this theory to a specific example. These objectives have been achieved by obtaining the following results:

- A nonlinear filtering lower bound algorithm has been derived based on Cramér-Rao theory. This algorithm yields most useful results at high SNR.

- A nonlinear filtering lower bound algorithm has been derived based on rate distortion theory. This algorithm yields most useful results at low SNR.

- A stochastic state-space model characterizing the dynamics of the surveillance problem has been developed.

- A computer program has been written which implements the low as well as the high SNR lower bound algorithms and the state-space model equations.

- Using this computer program, <u>range a.d bearing rms estimation performance</u> has been analyzed and the <u>sensitivity</u> to key parameters and conditions* has been evaluated.

A typical example of the numerical results obtained is shown in Fig. 5-1. In this figure, rms range error, as given by the Cramér-Rao (CR)-based and the rate-distortion-based bounds derived in this study, is plotted against SNR for three conditions: zero array distortion, array distortion with rms distortion of 2λ (i.e., twice the wavelength), and

R—51035
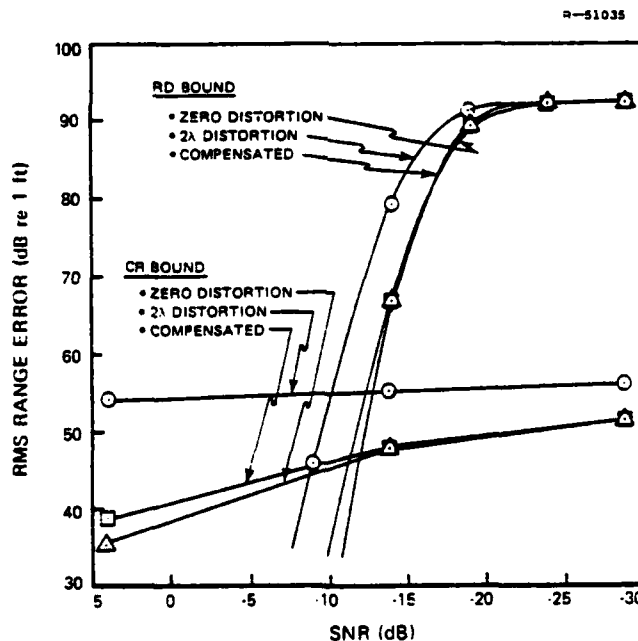
Figure 5-1   Effect of Array Distortion and Motion Compensation on Range Error as a Function of SNR

---

*SNR, RMS magnitude of towed array distortions, accuracy of motion compensation, magnitude of initial nominal range, initial target location uncertainty, integration of hull-mounted sonar and towed array measurements.

array distortion compensated with a gyrocompass-EM log instrumentation suite. The curves plotted show that <u>the RD-based bound is significantly tighter at low SNR whereas the CR-based bound is significantly tighter at high SNR</u>. The curves also indicate that significant performance improvement can be obtained by using the gyrocompass-EM log motion compensation instrumentation suite. <u>Other numerical results obtained (not shown in Fig. 5-1) demonstrate the possible pitfalls of applying linearized analysis to nonlinear problems such as the surveillance problem considered here (see Section 4.4).</u>

This report summarizes the results obtained to date in the current contract. Documentation providing in-depth technical details has been prepared in the form of TASC Technical Information Memorandums and open-literature publications (Refs. 12, 13, 14, 15, and 43).

REFERENCES

1. Marsh, J.A. and Stahmer, N.B., "THIN-LINE Array Technol-
    ogy Development: FY'74 Annual Report (U)," Naval Under-
    water Systems Center Technical Report No. 49.17, 30
    April 1975 (CONFIDENTIAL).

2. Newman, H.S., "Optimum Frequency and Processing Type
    for the TARP Localization Array (U)," 32nd Navy Sympo-
    sium on Underwater Acoustics, New London, Conneticut,
    14-16 November 1978 (SECRET).

3. Moura, J.M.F., Van Trees, H.L., and Baggeroer, A.B.,
    "Space-Time Tracking by a Passive Observer," 4th Symp.
    on Nonlinear Estimation Theory and Its Applications,
    San Diego, CA, September 1973.

4. Moura, J.M.F., and Baggeroer, A.B., "Passive Systems
    Theory with Narrow-Band and Linear Constraints: Part
    I," IEEE J. Oceanic Eng., Vol. OE-3, No. 1, January
    1978.

5. Moura, J.M.F., "Passive Systems Theory with Narrow-Band
    and Linear Constraints: Part II," IEEE J. Oceanic Eng.,
    Vol. OE-4, No. 1, January 1979.

6. Bangs, W., and Schultheiss, P.M., "Space-Time Process-
    ing for Optimal Parameter Estimation," in Signal Process-
    ing, edited by J.W.R. Griffiths et. al., Academic Press,
    New York, 1973.

7. Hahn, W.R., "Optimum Signal Processing for Passive Sonar
    Range and Bearing Estimation," J. Acoust. Soc. Am.,
    Vol. 58, No. 1, July 1975.

8. Carter, G.C., "A Brief Description of the Fundamental
    Difficulties in Passive Ranging," IEEE J. Oceanic Eng.,
    Vol. OE-3, No. 3, July 1978.

9. Carter, G.C., "Passive Ranging Errors Due to Receving
    Hydrophone Position Uncertainty," J. Acoust. Soc. Am.,
    Vol. 65, No. 2, February 1979.

10. Galdos, J.I., "A Lower Bound on Filtering Error with
    Application to Phase Demodulation," IEEE Trans. on Infor-
    mation Theory, Vol. IT-25, No. 4, July 1979.

REFERENCES (Continued)

11. Galdos, J.I., D'Appolito, J.A., and Mottl, T.O., "Instrumentation and Data Processing Techniques for Sensing Geometry Distortions in Towed Arrays," The Analytic Sciences Corporation Report No. TR-1333-1, 31 October 1978.

12. Lee, T.S., and Galdos, J.I., "State-Space Models for Sonar System Analysis," The Analytic Sciences Corporation Technical Information Memorandum TIM-1519-3.

13. Galdos, J.I., "A Cramér-Rao Bound for Multidimensional Discrete-Time Systems," The Analytic Sciences Corporation Technical Information Memorandum TIM-1519-1. Also IEEE Trans. on Auto. Control, Vol. AC-25, No. 1, Feb. 1980.

14. Galdos, J.I., "A Rate Distortion Theory Lower Bound on Desired Function Filtering Error," The Analytic Sciences Corporation Technical Information Memoradum TIM-1519-2. Also to appear in the IEEE Trans. on Info. Theory.

15. Galdos, J.I., and Lee, T.S., "Nonlinear Filtering Lower Bound Evaluation of Passive Tracking Systems," to appear in the Proceedings of the IEEE Intl. Conference on Acoustics, Speech and Signal Proc., Denver, April 1980.

16. Gelb, A., ed., Applied Optimal Estimation, M.I.T. Press, Cambridge, MA, 1974.

17. Urick, R.J., Principles of Underwater Sound for Engineers, McGraw-Hill, New York, 1975.

18. Cavanaugh, R.C., "Acoustic Fluctuation Modeling and System Performance Estimation Vol. I," Science Applications, Inc. Report No. SAI-79-737-WA, January 1978.

19. Axelrod, E.H., Schoomer, B.A., and Von Winkle, W.A., "Vertical Directionality of Ambient Noise in the Deep Ocean at a Site Near Bermuda," J. Acoust. Soc. Am., Vol. 37, No. 1, January 1965.

20. Dyer, I., "Statistics of Distant Shipping Noise," J. Acoust. Soc. Am., Vol. 53, No. 2, February 1973.

21. Singer, R.A., "Estimating Optimal Tracking Filter Performance for Manned Maneuvering Targets," IEEE Trans. on Aerospace and Electronic Systems, Vol. AES-6, No. 4, July 1970.

REFERENCES (Continued)

22. Bass, R.W., et al., "ASW Target Motion and Measurement Model," CSA Technical Report TR-72-024-01, 1 September 1972.

23. Moose, R.L., Vanlandingham, H.F., and McCabe, D.H., "Modeling and Estimation for Tracking Maneuvering Targets," IEEE Transactions on Aerospace and Electronic Systems, Vol. AES-15, No. 3, May 1979.

24. Kennedy, R.M., "Transverse Motion Response of a Cable Towed Array System; Part I, Theory," USN J. Underwater Acoustics, January 1980.

25. Ortloff, C.R., and Ives, J., "On the Dynamic Motion of a Thin Flexible Cylinder in a Viscous System," J. Fluid Mech., Vol. 38, Part 4, April 1969.

26. McDonald, V.H., and Schultheiss, P., "Optimal Passive Bearing Estimation in a Spatially Incoherent Noise Environment," J. Acoust. Soc. Am., Vol. 46, No. 1, January 1969.

27. Van Trees, H.L., Detection, Estimation, and Modulation Theory Part I, Wiley, New York, 1968.

28. Papoulis, A., Probability, Random Variables, and Stochastic Processes, McGraw-Hill, New York, 1965.

29. Jazwinski, A.H., Stochastic Processes and Filtering Theory, Academic Press, 1970.

30. Seidman, L.P., "Performance Limitations and Error Calculations for Parameter Estimation," Proc. IEEE, Vol. 58, May 1970.

31. Sakrison, D.J., Notes on Analog Communication, New York: Van Nostrand, 1970.

32. Fortmann, T., and Baron, S., "Problems in Multi-Target Sonar Tracking," Proc. 1978 IEEE Conf. on Decision and Control, San Diego, CA, Jan. 1979.

33. Paidoussis, M.P., "Dynamics of Flexible Slender Cylinders in Axial Flow, Part 1: Theory," J. Fluid Mech., Vol. 26, Part 4, 1966.

REFERENCES (Continued)

34.   Baggeroer, A.B., "Sonar Signal Processing," in _Applica-
        tions of Digital Signal Processing_, A.V. Oppenheim,
        ed., Prentice-Hall, Englewood Cliffs, N.J., 1978.

35.   Gallager, R.G., _Information Theory and Reliable Communi-
        cation,_ New York: Wiley, 1968.

36.   Berger, T., _Rate Distortion Theory_, Englewood Cliffs,
        N.J., Prentice-Hall, 1971.

37.   Galdos, J.I.,and O'Halloran, W.F., "Performance Lower
        Bound Evaluation on Frequency Acquisition Filters,"
        Proc. 1978 IEEE Conf. on Decision and Control, San Diego,
        CA, Jan. 1979.

38.   Loeve, M., _Probability Theory_, Princeton, N.J., Van
        Nostrand, 1963.

39.   Bobrovsky, B.Z. and Zakai, M., "A Lower Bound on the
        Estimation Error for Markov Processes," _IEEE Trans.
        Automat. Contr._, Vol. AC-20, Dec. 1975.

40.   Kendall, M.G., and Stuart, A., _The Advanced Theory of
        Statistics_, Hafner Publishing Company, New York, 1969.

41.   Scott, D.W., "Nonparametric Probability Density Estima-
        tion by Optimization Theoretic Techniques," Rice Univers-
        ity Technical Report 476-131-1, Houston, Texas, 1976.

42.   International Mathematical and Statistical Libraries
        Reference Manual, IMSL Report LIB1-0006, Houston, Texas,
        1977.

43.   Galdos, J.I., and Lee, T.S., "Analysis of a Passive
        Tracking System," to be submitted to _IEEE J. Oceanic Eng._

44.   Schultz, D.G., and Melsa, J.L., _State Functions and Linear
        Control Systems_, McGraw-Hill, New York, 1967.

UNCLASSIFIED

REPORT DOCUMENTATION PAGE		READ INSTRUCTIONS BEFORE COMPLETING FORM
1. REPORT NUMBER TR-1519-1	2. GOVT ACCESSION NO. AD-A085 671	3. RECIPIENT'S CATALOG NUMBER
4. TITLE (and Subtitle) Performance Lower Bounds for Compensated Tracking Sensors		5. TYPE OF REPORT & PERIOD COVERED Interim Technical Report Sept. 1978 — Feb. 1980
		6. PERFORMING ORG. REPORT NUMBER TR-1519-1
7. AUTHOR(s) Jorge I. Galdos and T. Sen Lee		8. CONTRACT OR GRANT NUMBER(s) N00014-78-C-0684
9. PERFORMING ORGANIZATION NAME AND ADDRESS The Analytic Sciences Corporation Six Jacob Way Reading, Massachusetts 01867		10. PROGRAM ELEMENT. PROJECT. TASK AREA & WORK UNIT NUMBERS 65152N RO145 TW NP. 274-301
11. CONTROLLING OFFICE NAME AND ADDRESS Naval Analysis Program (Code 431) Office of Naval Research Arlington, Virginia 22217		12. REPORT DATE 28 February 1980
		13. NUMBER OF PAGES 57
14. MONITORING AGENCY NAME & ADDRESS(if different from Controlling Office) DCASMA, Boston 666 Summer Street Boston, MA 02210		15. SECURITY CLASS. (of this report) UNCLASSIFIED
		15a. DECLASSIFICATION/ DOWNGRADING SCHEDULE

16. DISTRIBUTION STATEMENT (of this Report)

"Approved for Public Release; distribution unlimited"

17. DISTRIBUTION STATEMENT (of the abstract entered in Block 20, if different from Report)

18. SUPPLEMENTARY NOTES

19. KEY WORDS (Continue on reverse side if necessary and identify by block number)

Sonar, Tracking, Surveillance, Localization, Nonlinear Filtering, Optimal Estimation, Lower Bounds, Cramer-Rao, Rate Distortion Theory, Performance Evaluation, Towed Arrays, Hull-mounted Sonar, State Space Model

20. ABSTRACT (Continue on reverse side if necessary and identify by block number)

(see reverse side)

DD $_{1 \text{ JAN } 73}^{\text{FORM}}$ 1473   EDITION OF 1 NOV 65 IS OBSOLETE

UNCLASSIFIED

Block 20.   (Abstract)

The process of tracking and localization of a moving
acoustic source in the ocean has a natural formulation as a
problem in nonlinear filtering theory. In general, the op-
timal estimator for this signal processing problem cannot
be explicitly constructed nor can optimal performance be
computed. However, optimal performance can be approximated
by using mathematical algorithms which provide lower bounds
on attainable estimation accuracy. Lower bound on tracking
and localization errors are especially useful in that they
indicate system performance limits and can be computed from
basic measurement scenario parameters without reference to
specific estimator structure. This report describes the
mathematical structure and software required to compute
nonlinear filtering lower bounds to the tracking and local-
ization performance attainable with a towed linear acoustic
array and a hull-mounted sonar. The state-space model for
the acoustic environment and sensor measurement processes
used by the lower bound algorithms is also described. Range
and bearing estimation performance as a function of signal-
to-noise ratio, array distortion, and other important param-
eters, is studied for a generic measurement scenario.

Distribution List for
"A Multi-Target Survey"
Volumes I & II

NAME	NUMBER OF COPIES
Defense Technical Information Center Cameron Station Alexandria, VA 22314	12
Center for Naval Analyses 2000 North Beauregard Street Alexandria, VA 22311	1
Office of Naval Research Code 431 Arlington, VA 22217	2
Dr. Byron D. Tapley The University of Texas at Austin Department of Aerospace Engineering and Engineering Mechanics Austin, TX 78712	1
Dr. Fred W. Weidmann TRACOR, Inc. Tracor Sciences & Systems 6500 Tracor Lane Austin, TX 78721	1
Naval Postgraduate School Technical Library Monterey, CA 93940	1
Naval Underwater Systems Center New London Laboratory Code 313 Code 333 New London, CT 06320	1 1
Naval Underwater Systems Center Code 352 Newport, RI 02840	1
Dr. J. Anton Systems Control, Inc. 1801 Page Mill Road Palo Alto, CA 94304	1
Office of Naval Research Eastern Regional Office 666 Summer Street Boston, MA 02210	1

Name	Number of Copies
Naval Ocean Systems Center Code 7131 San Diego, CA 92152	1
Naval Surface Weapons Center White Oak Laboratory Code U-20 Silver Spring, MD 20910	2
Dr. Yaakov Bar-Shalom The University of Connecticut Department of Electrical Engineering and Computer Science Box U-157 Storrs, CT 06268	1
Mr. Conrad Naval Intelligence Support Center Code 20 Suitland, MD 20390	1
Dr. V. T. Gabriel General Electric Company Sonar Systems Engineering Farrell Road Plant Building 1, Room D6 Syracuse, NY 13201	1
Naval Air Development Center Warminster, PA 18974	1
Naval Electronics Systems Command Washington, DC 20360 Code 320 PME-124	1 1
Naval Research Laboratory Washington, DC 20375 Code 2627 Code 5308 Code 7932	6 1 1
Naval Sea Systems Command Washington, DC 20360 Code 63R-1 Code 63R-16 Code 63G	1 1 1
Dr. R. Moose Department of Electrical Engineering Virginia Polytechnic Institute Blacksburg, VA 24061	1